

MedChemComm

Accepted Manuscript



This is an *Accepted Manuscript*, which has been through the Royal Society of Chemistry peer review process and has been accepted for publication.

Accepted Manuscripts are published online shortly after acceptance, before technical editing, formatting and proof reading. Using this free service, authors can make their results available to the community, in citable form, before we publish the edited article. We will replace this *Accepted Manuscript* with the edited and formatted *Advance Article* as soon as it is available.

You can find more information about *Accepted Manuscripts* in the [Information for Authors](#).

Please note that technical editing may introduce minor changes to the text and/or graphics, which may alter content. The journal's standard [Terms & Conditions](#) and the [Ethical guidelines](#) still apply. In no event shall the Royal Society of Chemistry be held responsible for any errors or omissions in this *Accepted Manuscript* or any consequences arising from the use of any information it contains.

3,5-Diamino-1,2,4-triazoles as a novel scaffold for potent, reversible LSD1 (KDM1A) inhibitors

Cite this: DOI: 10.1039/x0xx00000x

Craig J. Kutz,^{a§} Steven L. Holshouser,^{a§} Ethan A. Marrow^a and Patrick M. Wooster^{a*}

Received 00th January 2012,
Accepted 00th January 2012

DOI: 10.1039/x0xx00000x

www.rsc.org/

The chromatin remodeling amine oxidase lysine-specific demethylase 1 (LSD1) has become an attractive target for the design of specific inhibitors with therapeutic potential. We, and others, have described LSD1 inhibitors that have potential as antitumor agents. Many of the currently known LSD1 inhibitors are poor drug candidates, or are structurally based on the tranylcypromine backbone, thus increasing the potential for off-target effects mediated by other amine oxidases. We now describe a series of potent LSD1 inhibitors based on a novel 1,2,4-triazole scaffold; these inhibitors show a high degree of specificity for LSD1 in vitro, and cause increases in cellular histone 3 dimethyllysine 4 (H3K4me2), a gene transcription activating mark. Importantly, these inhibitors are not toxic to mammalian cells in vitro, and thus they may show utility in the treatment of epigenetically-based diseases where cell death is not a desired endpoint

INTRODUCTION

The dynamic interplay between histones and chromatin remodeling is critical for selective control of gene expression, and chromatin remodeling enzymes have now become attractive therapeutic targets for multiple diseases with an epigenetic basis. A number of post-translational histone modifications are known to control gene expression, including methylation, ubiquitination, sumoylation, ADP-ribosylation and acetylation of histone lysine or arginine residues, ADP-ribosylation of glutamate residues and phosphorylation of histone serine residues.¹ The FAD-dependent amine oxidase lysine-specific demethylase 1 (LSD1, also known as KDM1A or BHC110) bound to the co-repressor CoREST, preferentially demethylates the mono- and dimethylated forms of the activating mark histone 3 lysine 4 (H3K4) to repress gene transcription.^{2, 3} Under some conditions (e.g. when bound to the androgen receptor), LSD1 also demethylates the mono- and dimethylated forms of the deactivating chromatin mark H3K9.⁴ Because LSD1 is overexpressed in a number of human cancers (acute myeloid leukemia, neuroblastoma, retinoblastoma, prostate cancer, breast cancer, lung cancer and bladder cancer),⁵⁻⁸ the protein has emerged as an important target for the development of specific inhibitors as a new class of antitumor agents.⁹ Importantly, LSD1 is now regarded as an emerging drug target for diseases other than cancer, such as neurological disease,^{10, 11} blood disorders,^{12, 13} viral

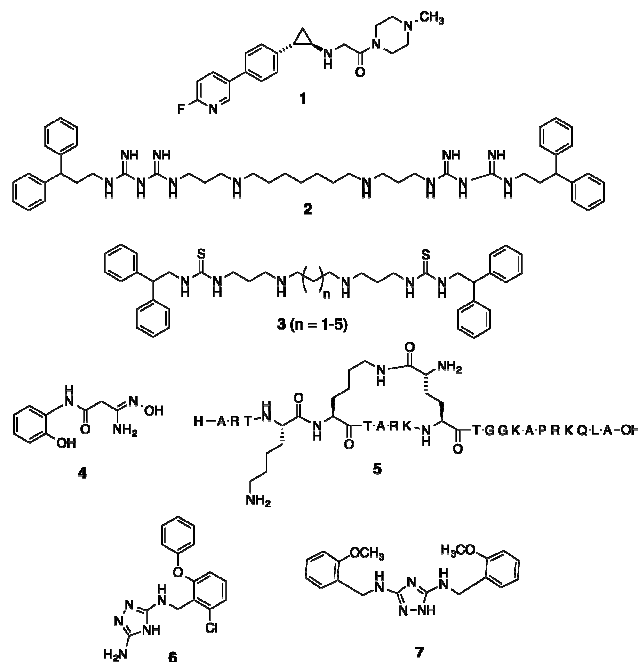


Figure 1. Structures of LSD1 inhibitors **1**, verindamycin **2**, (bis)thioureas **3**, amidoxime **4**, cyclic peptide **5**, N³-(2-chloro-6-phenoxybenzyl)-4H-1,2,4-triazole-3,5-diamine **6** and N³,N⁵-bis(2-methoxybenzyl)-1H-1,2,4-triazole-3,5-diamine **7**.

infection,¹⁴ diabetes^{15, 16} and fibrosis.¹⁷ As such, there is a need for potent epigenetic modulators that do not cause overt cytotoxicity.

To date, a number of small molecule inhibitors of LSD1 have been described, as shown in Figure 1. Effective LSD1 inhibitors include tranylcypromine-based analogues^{3, 18-20} such as **1**,²¹ oligoamines such as verlindamycin **2**²² and related isosteric ureas and thioureas related to **3**,^{23, 24} small-molecule amidoximes such as **4**,²⁵ and peptide based LSD1 inhibitors such as **5**.^{26, 27} Many of the most potent and selective LSD1 inhibitors are structurally based on the clinically used antidepressant tranylcypromine, which has an IC₅₀ value of 20.7 μ M for LSD1. Because tranylcypromine is a potent inhibitor of monoamine oxidases and other flavin-dependent amine oxidases, there is a potential for undesired off-target effects in tranylcypromine-based LSD1 inhibitors. In addition, compounds built on a tranylcypromine scaffold rely on covalent, irreversible adduct formation with FAD to inactivate the enzyme. Herein we describe a novel scaffold for a new series of reversible, competitive inhibitors of LSD1, the 3,5-diaminotriazole moiety. The 3,5-diaminotriazole scaffold was used to produce histone demethylase inhibitors exhibiting increased potency for LSD1 (IC₅₀ 1-2 μ M), higher specificity when compared to monoamine oxidase A and B (IC₅₀ values > 100 μ M), and reduced cytotoxicity. These analogues have great therapeutic potential for treatment of cancer, and importantly, for use in other epigenetically driven disorders where cytotoxicity is not a desired endpoint.

RESULTS

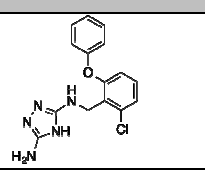
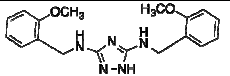
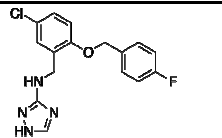
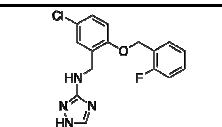
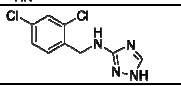
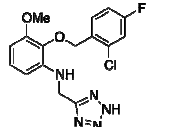
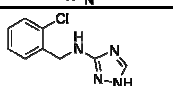
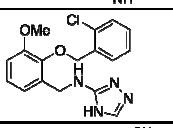
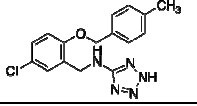
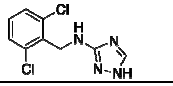
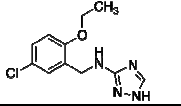
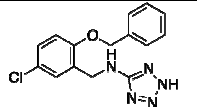
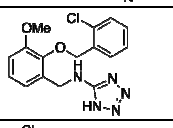
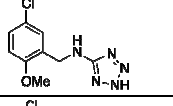
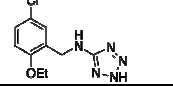
Virtual screen for novel LSD1 inhibitors

Potential new scaffolds for small-molecule LSD1 inhibitors were identified through a virtual screen of the Maybridge Hitfinder 5 compound library, as previously described.²⁵ The crystal structure of LSD1/CoREST (PDB 2V1D) was prepared using PrepWizard, and SiteMap was then used to assess efficient binding within the LSD1 histone-binding pocket. Lowest energy conformers of 3D compounds were determined and docked in the LSD1 active site using Glide. A total of 10 hits were identified with Glide scores lower than -7.5 kcal/mol. The synthesis and biological evaluation of other lead compounds identified in this screen have been previously published.²⁵ In the present study, two hits from the virtual screen, compounds **6** and **7** (Figure 1), were identified, and these compounds, as well as related analogues **8-20**, were purchased and evaluated (Table 1).

In vitro activity against recombinant LSD1/CoREST

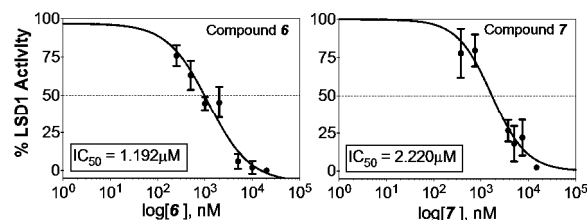
The ability of compounds **6-20** to inhibit purified recombinant LSD1 was measured using a commercially available fluorescence-based assay kit (Cayman Chemicals #700120). Initially, all compounds were tested at a concentration of 10 μ M in phosphate-buffered saline (PBS) containing <1% DMSO (Table 1). The screen was performed as suggested by the supplier and modified as previously described.^{23, 25} Compounds **6** and **7** were the most effective

Table 1. Structures, cLogP and LSD1 inhibitory activity for 3,5-diaminotriazoles **6-20**. Each data point is the average of 3 determinations \pm standard error of the mean.

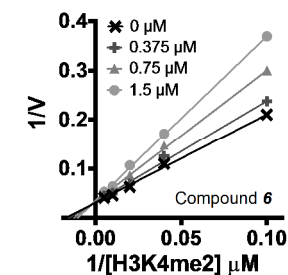
Structure	Cmpd.	cLogP	Residual % LSD1 Activity (I) 10 μ M
	6	3.73	15.1 \pm 4.7
	7	3.58	25.1 \pm 1.9
	8	4.46	72.3 \pm 9.0
	9	4.46	69.4 \pm 6.4
	10	3.21	97.8 \pm 6.9
	11	2.90	103.1 \pm 7.8
	12	2.49	95.4 \pm 6.9
	13	3.648	81.9 \pm 8.2
	14	3.53	93.1 \pm 7.5
	15	3.21	69.1 \pm 7.7
	16	3.08	103 \pm 12.7
	17	3.03	80.1 \pm 8.4
	18	2.62	77.9 \pm 7.3
	19	1.27	69.2 \pm 5.7
	20	1.795	79.2 \pm 5.0

inhibitors of LSD1 (%LSD1 activity remaining 15.1 ± 4.7 and 25.1 ± 1.9 , respectively). For comparison, tranlycypromine (TCP) and compound **2** reduced LSD1 activity to 72.6 and 15.8%, respectively. Compounds **6** and **7** were then subjected to titration analysis to determine the *in vitro* IC_{50} of each compound against LSD1 (Figure 2, Panel A). Compound **6** possessed an IC_{50} value of $1.19 \mu\text{M}$ while compound **7** had an IC_{50} value of $2.22 \mu\text{M}$.

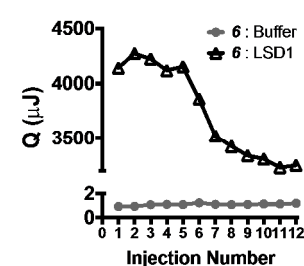
Panel A



Panel B



Panel C



Panel D

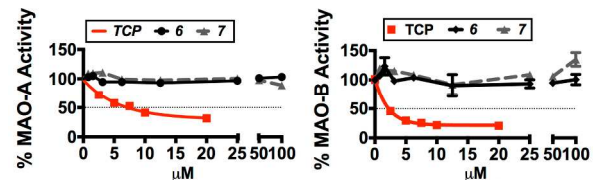


Figure 2. Potency, inhibition kinetics, binding and selectivity of 3,5-diaminotriazoles **6 and **7**.** Panel A. Dose-response of LSD1 following treatment with compounds **6** and **7**. Compound **6** $IC_{50} = 1.19 \mu\text{M}$; compound **7** $IC_{50} = 2.22 \mu\text{M}$ Panel B. Competitive enzyme inhibition kinetics for LSD1 treated with compound **6** at 0, 0.375, 0.75, and $1 \mu\text{M}$ concentrations over a range of substrate concentrations between 0 and $100 \mu\text{M}$. K_i for **6** = $2.2 \mu\text{M}$ Panel C. Isothermal calorimetry trace for LSD1 showing a release of heat upon titration with compound **6**. $K_a = 48.89 \text{ nM}$, $R^2 = 0.96$ Panel D. MAO A and MAO B enzyme activity for 3,5-diaminotriazoles **6** and **7** compared to the known MAO inhibitor tranlycypromine (TCP). TCP $IC_{50} = 4.2 \mu\text{M}$ and $5.8 \mu\text{M}$ for MAO A and MAO B, respectively). Compounds **6** and **7** exhibited IC_{50} values $> 100 \mu\text{M}$ for both MAO A and B. For Panels A, B and D, each data point is the average of 3 determination that in each case differed by 3% or less.

Compound **6** is a reversible, competitive inhibitor of LSD1

The fluorescence-based assay method described above was then used to determine Michaelis-Menten kinetics for **6**, as shown in Figure 2, Panel B. In brief, compound **6** was incubated at 0, 0.375, 0.75 and $1.0 \mu\text{M}$ for 30 mins with 15

$\text{ng}/\mu\text{L}$ of LSD1 at 37°C prior to addition of increasing amounts of the H3K4me2 peptide substrate (concentrations between 0 and $100 \mu\text{M}$). Initial rates were determined by linear least-squares fit, and K_m and V_{max} values were determined using the GraphPad Prism 6 software package. The V_{max} remained constant ($30.62 \pm 0.8 \text{ unit}/\text{min}$) indicating competitive inhibition, and the K_i for **6** was determined to be $2.20 \mu\text{M}$.

To assure that 3,5-diaminotriazoles were bound to LSD1 with 1:1 stoichiometry, nanoisothermal titration calorimetry (ITC) was performed (Figure 2, Panel C) using compound **6** and purified LSD1 (Enzo Life Sciences, #BML-SE544-0050). Titration of compound **6** to LSD1 resulted in an independent binding isotherm signifying significant heat release on binding of **6** to LSD1. The R^2 of heat released and the molar ratio was found to be 0.96.

Amine oxidase selectivity of 3,5-diaminotriazoles

LSD1 and other amine oxidases, such as the monoamine oxidases (MAO), use the cofactor FAD to reoxidize molecular oxygen to produce H_2O_2 . Tranlycypromine and derivatives often show significant off-target efficacy against MAO/A and MAO/B. A commercial recombinant luminescent assay (Promega Corporation, #V1401) was performed as described by the manufacturer to assess the ability of 3,5-diaminotriazole **6** and **7** to inhibit monoamine oxidase (MAO) A and B isoforms. Compounds **6** and **7** were diluted in 1% DMSO prior to measuring the activity of MAO A and B. Compounds **6** and **7** both exhibited IC_{50} values greater than $100 \mu\text{M}$ against both MAO isoforms, while tranlycypromine inhibited MAO A and B with IC_{50} values of $4.2 \mu\text{M}$ and $5.8 \mu\text{M}$, respectively (Figure 2D).

Molecular modeling studies for compound **6**

In silico molecular modeling (GOLD software package, version 5.1, Cambridge Crystallographic Data Center, Cambridge, UK) was performed to predict key residues interacting with compound **6** (Figure 3) and compound **7** (data not shown). The LSD1 active site (PDB #3ZMT, LSD1-CoREST in complex with a peptide with the sequence PRSFLV) was defined as a sphere enclosing residues within 10 \AA around the crystallographic peptide ligand. Prior to energy minimization, proteins were protonated and the pH was set to 7.4. Initial screens focused on using the PRSFLV peptide for defining potential key interaction sites. The 3D inhibitor structures were energy minimized using the MM94x force field for 1000 iterations and a convergence value of $0.001 \text{ kcal}/\text{mol}/\text{\AA}$ as the termination criterion. Initial docking results yielded 60 poses of each structure bound in the active site of LSD1. The top 5 poses that yielded the lowest E-score were chosen for further analysis. The best fit for binding was analyzed for interacting residues. Key interactions with compound **6** include two hydrogen bonds with aspartate 555 and another hydrogen bond with the carbonyl of alanine 539. In addition, the compound participates in pi-stacking with the flavin ring of the FAD cofactor within 2.98 \AA . Thus, compound **6** shows close association with the active site and effectively prohibits substrate binding. A 2-dimensional rendition of the

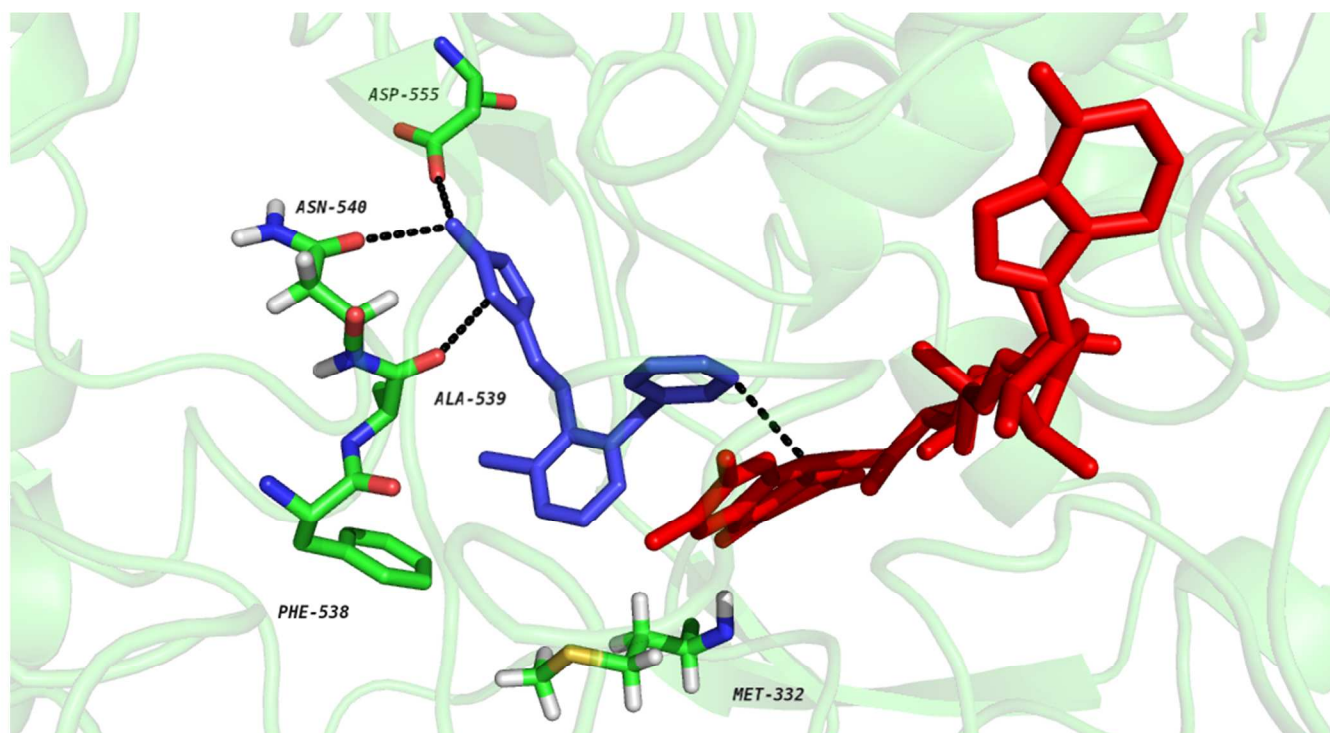


Figure 3. *In silico* analysis of compound **6** in the LSD1/CoREST catalytic site (PDB file 3ZMT). The aromatic portion of the *o*-phenoxy substituent lies 2.98Å from the FAD cofactor.

binding of **6** to LSD1/CoREST appears in the supplement, Figure S1.

Cytotoxicity, Cellular Effects, and Global H3K4me2 Levels

Calu-6 human lung adenocarcinoma cells were purchased from ATCC (HTB-56), and cultured in EMEM growth medium containing 10% (v/v) fetal bovine serum and 5% penicillin and streptomycin. Cultures were grown at 37°C in a humidified environment containing 5% CO₂. The cells were plated and maintained in a clear bottom, 96 well plate and seeded at 1,000 cells/ well. After attachment, the cells were

dissolved in DMSO and then further diluted with culture medium. The cells were exposed to DMSO concentrations of less than 1%, and 1% DMSO was used as a negative control for cell growth. The known LSD1 inhibitor verlindamycin **2** was used as a positive control. Cells were fixed with 4% PFA, permeabilized with 1% Triton-X100 and stained with DAPI at 1:1000 with in PBS. As shown in Figure 4, compounds **6** and **7** were not cytotoxic to cultured Calu-6 lung tumor cells (IC₅₀ values > 100 µM), while **2** was cytotoxic with an IC₅₀ value of 5 µM. TCP was also not cytotoxic in the Calu-6 cell line at concentrations up to 100 µM, and in fact did not cause significant cytotoxicity at much higher concentrations (Figure S2).

The cytotoxicity of **6** and **7** was examined in 5 additional cell lines including CA46 Burkitt's lymphoma, the PC3 human prostate cancer cell line, the PANC1 human pancreatic cell line, the MDA-MB-231 estrogen receptor-negative cell line and the MCF-10A human breast epithelial cell line. LSD1 has been shown to be overexpressed in the PC3, PANC1 and MDA-MB-231 cell lines. Compounds **6** and **7** produced no significant cytotoxicity in the CA46 and MCF-10A lines, although **6** had an IC₅₀ of 52 µM in the MCF-10A line. In the PC3 line, both **6** and **7** exhibited IC₅₀ values near 74 µM, compared to **2**, which produced 85% growth inhibition at 8 µM. In the PANC1 and MDA-MB-231 lines, **7** was not an effective growth inhibitor, with IC₅₀ values of 80 and 55 µM, respectively. Interestingly, compound **6** was an effective growth inhibitor in the PANC1 and MDA-MB-231 cell lines, exhibiting IC₅₀ values of 19 and 12 µM, respectively. The mechanism underlying this activity

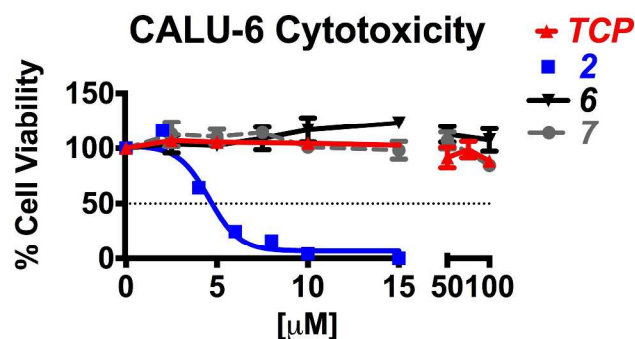


Figure 4. Cell viability and compound cytotoxicity in Calu-6. Cells were seeded at 3x10³ cells/well and treated 48-72hrs with increasing concentrations of TCP, **2**, **6** or **7**. Cell viability was determined by colorimetric CellTiter 96 Aqueous MTS (Promega, #G3580).

exposed to varying concentrations of the drug, while being kept in a humidified environment for 48 or 72 hours. Compounds

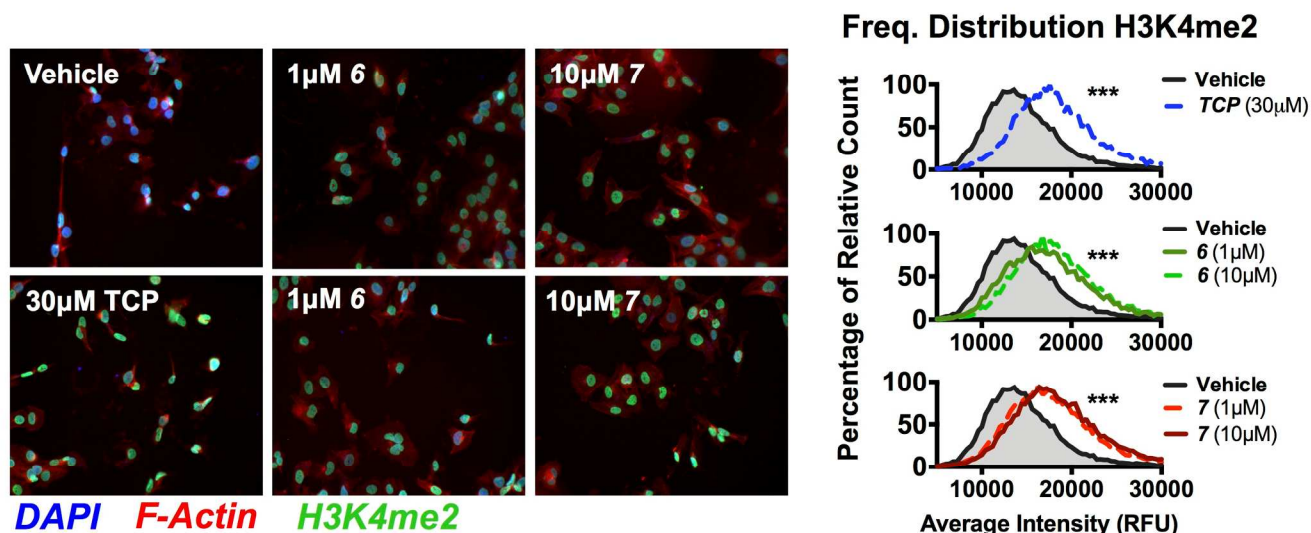


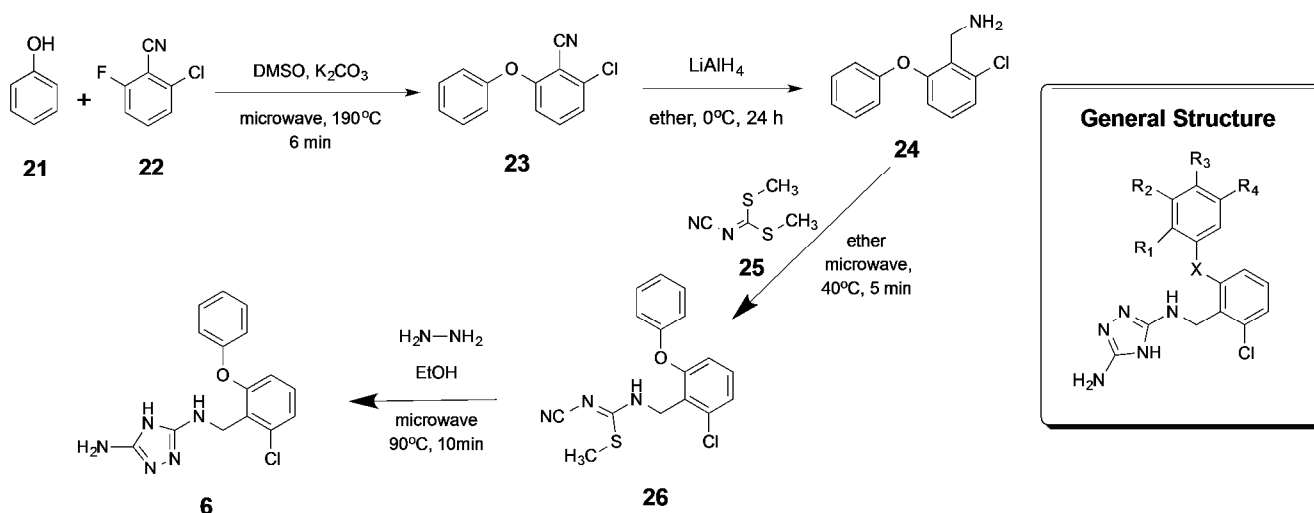
Figure 5. Global methylation changes by immunofluorescent staining. Calu-6 human lung adenocarcinoma cells were plated at 1×10^3 cells/well and treated with 30 μ M TCP, 1- or 10 μ M compound **6**, and 1- or 10 μ M compound **7** for 48 hrs. Cells were stained for nucleus (DAPI), F-actin (Alexa Fluor 594 Phalloidin), and dimethyl-H3K4 (Alexa Fluor 488 Secondary Antibody). Fluorescent intensity on cell-by-cell basis was obtained by Hermes WiScan (IDEA Biomedical) and graphed as a frequency distribution histogram of relative cell count at specific intensities. Two-way ANOVA; *** P-value < 0.001, representative of 3 experiments with n=4-6 wells each.

remains to be determined; however, it can be generally stated that **6** and **7** produce little cytotoxicity in multiple cell lines in vitro.

To measure the cellular effects of 3,5-diaminotriazoles **6** and **7**, treated cells from the cytotoxicity assay above were stained for immunofluorescence (IF) imaging using the appropriate fluorescently labelled secondary antibodies. In a 96-well plate, 5% BSA was added to specific wells and the plate was allowed to stand for 2 hours. The plate was then incubated at 4°C overnight with the primary antibody for H3K4me2 (Cell Signaling #2139S) diluted in 1% bovine serum albumin (BSA). Fluorescent secondary antibodies were then added to each well at 1:500 dilutions in 1% BSA for 2 hours. Cells were washed, suspended in PBS and viewed for intensity

of signal per cell (Hermes WiScan, Idea Biomedical). The imaging system is able to generate 10-40x images as well as quantify average intensity on a per-well basis, eliminating any bias towards IF staining. Compounds **6** and **7** at both 1 and 10 μ M developed green fluorescence in the nucleus at 48 hours that was comparable to the fluorescence promoted by 30 μ M tranylcypromine (Figure 5), indicating a significant increase in H3K4me2 levels. The H3K4me2 levels were quantified and graphed as cell count vs. average intensity (RFU) as shown in the histogram (Figure 5). The mean population intensity (MPI) \pm SEM for the vehicle was $1.44 \times 10^4 \pm 71$ RFU. By way of comparison, the MPI for 30 μ M TCP was $1.86 \times 10^4 \pm 136$ RFU (1.3-fold increase), for 10 μ M compound **6** $1.82 \times 10^4 \pm 105$ RFU (1.26-fold increase), and for 10 μ M compound **7** 1.91×10^4

Scheme 1



± 124 RFU (1.33-fold increase). Thus, compounds **6** and **7** at $1.0 \mu\text{M}$ were as effective as $30 \mu\text{M}$ TCP at increasing H3K4me2 levels in Calu-6 cells in vitro.

Synthesis of 3,5-diaminotriazole analogues

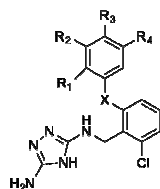
In order to produce additional analogues in the 3,5-diaminotriazole library, a synthesis of **6** was developed, as shown in Scheme 1. Condensation of phenol **21** and 2-cyano-3-chlorofluorobenzene **22** (K_2CO_3 , microwave, 190°C , 6 min) resulted in the phenoxyphenyl intermediate **23**. The cyano group in compound **23** was then reduced (LiAlH_4) to afford primary amine **24**, which was reacted with **25** (microwave, 40°C , 5 min) to yield **26**. Intermediate **26** was then treated with hydrazine (microwave, 90°C , 10 min) to produce the desired 3,5-diaminotriazole **6**. This route was used to synthesize the previously unreported 3,5-diaminotriazoles of the general structure shown in Scheme 1, compounds **27-42** (Table 2). Each compound was evaluated as an inhibitor of recombinant LSD1 as described above at a concentration of $10 \mu\text{M}$ (Figure 6). Six compounds (**6**, **7**, **32**, **35**, **37** and **39**) were more effective

LSD1 inhibitors at $10 \mu\text{M}$ than the known LSD1 inhibitor **2**, while 11 of the 16 compounds measured inhibited LSD1 by 50% or more. The small number of analogues shown in Table 2 are insufficient for the development of structure/activity relationships, however, the activity associated with **6**, **32**, **35**, **37** and **39** suggests that activity is retained with the addition of small electron releasing groups to the phenoxy aromatic ring at positions $\text{R}_1\text{-R}_4$. Compounds **37** and **39**, which have LSD1 inhibitory activity comparable to **6**, have been selected for further study, and are being subjected to the bioevaluation studies described above. In addition, we are continuing to synthesize analogues in this series for the purpose of refining a structure/activity model for 3,5-diaminotriazole-based LSD1 inhibitors. These results will be reported in a subsequent publication along with the complete biological characterization of **37** and **39**.

Discussion

Newly identified roles for epigenetic modulation involving LSD1 continue to emerge, both in cancer and in other disease states, and thus, has become a promising target for therapeutic intervention. The TCP-based LSD1 inhibitors are the most advanced chemical class with respect to drug development, and the first clinical trial for a tranlycypromine-based LSD1 inhibitor for treatment of acute myeloid leukemia began earlier this year.²⁸ TCP is a moderately potent, irreversible inhibitor of LSD1 and continues to provide a popular scaffold for the design of clinically relevant LSD1 inhibitors. However, it is challenging to design a TCP-based LSD1 inhibitor for clinical use that is specific, has low toxicity, and is devoid of the many biological responses to TCP itself. Thus, these analogues have the potential to produce off-target effects mediated through

Table 2. Structures, cLogP and LSD1 residual activity for 3,5-diaminotriazoles **2**, **6**, **7** and **27-42** at $10 \mu\text{M}$. Each data point is the average of 3 determinations \pm standard error of the mean. Compounds **34** and **36** were insoluble and thus were not screened for LSD1 inhibition. TCP = tranlycypromine



#	X	R ₁	R ₂	R ₃	R ₄	cLogP	% LSD1 Activity (10 μM)
TC P	-	--	--	--		--	64.2 \pm 6.1
2	-	--	--	--		--	33.9 \pm 6.7
6	-	H	H	H	H	3.73	15.1 \pm 4.7
7	-	--	--	--	--	3.58	25.1 \pm 1.9
27	O	H	H	CF ₃ O	H	5.47	61.4 \pm 5.6
28	O	H	H	CH ₃	H	4.94	40.7 \pm 6.1
29	O	(CH ₃) ₂ C H	H	H	CH ₃	5.97	43.7 \pm 3.2
30	O	H	CH ₃ O	H	H	4.36	55.4 \pm 5.1
31	O	H	H	(CH ₃) ₃ C	H	6.27	41.8 \pm 8.8
32	O	H	CH ₃	H	CH ₃	5.44	32.1 \pm 8.8
33	O	H	CF ₃	H	CF ₃	6.21	55.1 \pm 4.6
34	O	H	H	S-CF ₃	H	6.11	insolb.
35	O	CF ₃	H	Br	H	6.19	32.2 \pm 5.4
36	O	H	H	S-CH ₃	H	6.11	insolb.
37	O	CH ₃ O	H	CH ₃	H	4.51	15.3 \pm 3.2
38	O	H	CH ₃ O	H	CH ₃ O	4.45	36.7 \pm 8.6
39	O	CH ₃	CH ₃	H	H	5.39	19.4 \pm 1.9
40	O	H	O-CH ₂ -O		H	4.41	34.2 \pm 6.4
41	S	H	H	H	H	4.74	39.2 \pm 7.9
42	S	H	CH ₃ O	CH ₃ O	H	4.40	46.8 \pm 7.4

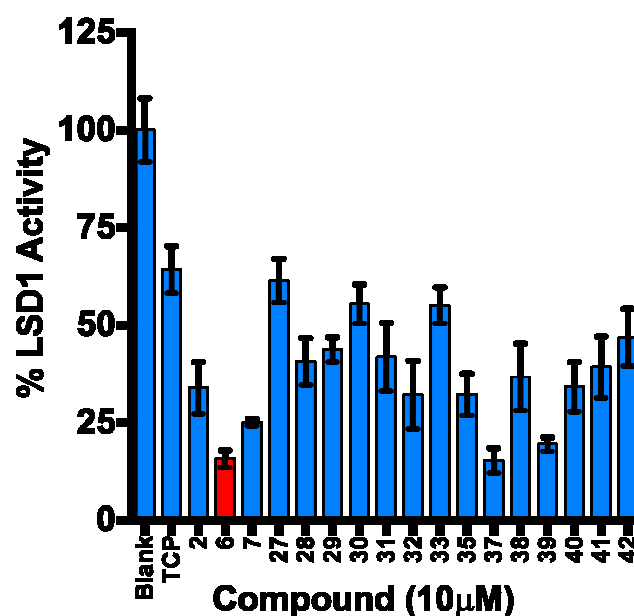


Figure 6. LSD1 inhibition assay. Percent LSD1 activity remaining after treatment with 3,5-diaminotriazoles **6**, **7**, **27-33**, **35**, **37-42** at $10 \mu\text{M}$. Each data point is the average of 3 determinations \pm SEM (see Table 2).

other flavin-dependent amine oxidase enzymes.²⁹ As such, there is a continuing need to identify novel small-molecule scaffolds for inhibitors of LSD1 that can be used to design highly specific LSD1 inhibitors. The 1,2,4-triazole moiety described in this manuscript could be used as such a scaffold, and the preliminary studies described herein support the contention that potent, non-toxic LSD1-specific inhibitors can be designed in this chemical class.

During the preparation of this manuscript, a series of 1,2,3-triazole-based LSD1 inhibitors were described.³⁰⁻³² In these analogues, the triazole ring system is derived from click chemistry used in their preparation, and is regioisomeric to the 1,2,4-triazoles described in this manuscript. Although the 1,2,3-triazole moiety contributes to binding to LSD1, the activity of the 1,2,3-triazoles depends on a dithiocarbamate moiety, and the compounds act as irreversible inactivators of LSD1.³² The compounds we have described in this report do not require activation and/or covalent attachment to the FAD cofactor for inhibition of LSD1, and our enzymatic kinetic studies have revealed that these compounds act as potent competitive inhibitors (Figure 2B). Thus, compounds **6** and **7** are among the first reversible small molecule compounds that possess selectivity for LSD1 over MAO A and B. Compounds **6** and **7** also produce the desired epigenetic effect, namely a significant increase in H3K4me2 levels, indicating that they enter mammalian cells and are active within the cell nucleus. The low level of toxicity to mammalian cells produced by **6** and **7** demonstrate that the 1,2,4-triazole scaffold can be used to produce LSD1 inhibitors that can be used in non-cancer disease states. As shown in Table 2, our early hit-to-lead studies suggest that we will be able to identify more potent analogues in the series. As such, the design, synthesis and evaluation of additional analogues related to **6** and **7** is an ongoing concern in our laboratories.

Conclusions

In summary, we have identified the 3,5-diamino-1,2,4-triazole nucleus as a novel scaffold for the design of nontoxic, reversible small molecule inhibitors of LSD1 that do not contain a tranylcypromine backbone. To our knowledge, compound **6** is one of the first small molecule, reversible LSD1 inhibitors that is active at low micromolar concentrations. There is a high probability that hit-to-lead and lead optimization studies will lead to more potent inhibitors that have high selectivity for LSD1, improved pharmacokinetic parameters and minimal off-target effects, and these studies are currently underway.

Acknowledgements

The research described in this manuscript was supported by NIH/NCI grant 5 RO1 CA149095 (PMW).

Notes and references

^a Department of Drug Discovery and Biomedical Sciences, College of Pharmacy, Medical University of South Carolina, 70 President St., Charleston, SC 29425.

[§]These authors contributed equally to the research described in this manuscript.

Electronic Supplementary Information (ESI) available: complete experimental section, including synthetic details and a description of all biological procedures.

1. F. Andreoli and A. Del Rio, *Drug Disc. Today* 2014, doi: 10.1016/j.drudis.2014.05.005. [Epub ahead of print].
2. Y. Shi, F. Lan, C. Matson, P. Mulligan, J. R. Whetstone, P. A. Cole, R. A. Casero and Y. Shi, *Cell* 2004, **119**, 941.
3. T. Suzuki and N. Miyata, *J. Med. Chem.* 2011, **54**, 8236.
4. R. A. Varier and H. T. Timmers, *Biochim. Biophys. Acta* 2011, **1815**, 75.
5. S. Hayami, J. D. Kelly, H. S. Cho, M. Yoshimatsu, M. Unoki, T. Tsunoda, H. I. Field, D. E. Neal, H. Yamaue, B. A. Ponder, Y. Nakamura and R. Hamamoto, *Int'l. J. Cancer* 2011, **128**, 574.
6. S. Lim, A. Janzer, A. Becker, A. Zimmer, R. Schule, R. Buettner and J. Kirfel, *Carcinogenesis* 2010, **31**, 512.
7. D. Rotili and A. Mai, *Genes & Cancer* 2011, **2**, 663.
8. J. H. Schulte, S. Lim, A. Schramm, N. Friedrichs, J. Koster, R. Versteeg, I. Ora, K. Pajtlar, L. Klein-Hitpass, S. Kuhfittig-Kulle, E. Metzger, R. Schule, A. Eggert, R. Buettner and J. Kirfel, *Cancer Res.* 2009, **69**, 2065.
9. P. Stavropoulos and A. Hoelz, *Exp. Op. Ther. Targets* 2007, **11**, 809.
10. J. M. Gottesfeld and M. Pandolfo, *Future Neurol.* 2009, **4**, 775.
11. B. Lakowski, I. Roelens and S. Jacob, *J. Mol. Neurosci.* 2006, **29**, 227.
12. G. D. Ginder, *Transl. Res.* 2014, epub ahead of print.
13. L. Shi, S. Cui, J. D. Engel and O. Tanabe, *Nat. Med.* 2013, **19**, 291.
14. Y. Liang, D. Quenelle, J. L. Vogel, C. Mascaro, A. Ortega and T. M. Kristie, *mBio*. 2013, **4**, e00558.
15. M. Mishra, Q. Zhong and R. A. Kowluru, *Free Rad. Biol. Med.* 2014.
16. D. Pan, C. Mao and Y. X. Wang, *PLoS ONE* 2013, **8**, e66294.
17. I. V. Yang and D. A. Schwartz, *Transl. Res.* 2014, epub ahead of print.
18. N. Guibourt, A. Ortega-Munoz and J. Castro-Palomino Laria, US Patent Application 20120004262: Phenylcyclopropylamine derivatives and their medical use. 2012.
19. S. Mimasu, N. Umezawa, S. Sato, T. Higuchi, T. Umehara and S. Yokoyama, *Biochemistry* 2010, **49**, 6494.
20. A. Ortega-Munoz, J. Castro-Palomino Laria and M. C. T. Fyfe Lysine-specific demethylase 1 inhibitors and their use. WO2011035941A1, 31 March 2011.
21. R. Neelamegam, E. L. Ricq, M. Malvaez, D. Patnaik, S. Norton, S. M. Carlin, I. T. Hill, M. A. Wood, S. J. Haggarty and J. M. Hooker, *ACS Chem. Neurosci.* 2012, **3**, 120.
22. Y. Huang, E. Greene, T. M. Stewart, A. C. Goodwin, S. B. Baylin, P. M. Woster and R. A. Casero, *Proc. Nat'l. Acad. Sci. USA* 2007, **104**, 8023.

23. S. Sharma, Y. Wu, N. Steinbergs, M. Crowley, A. Hanson, R. A. J. Casero and P. Woster, *J. Med. Chem.* 2010, **53**, 5197.
24. S. K. Sharma, S. Hazeldine, M. L. Crowley, A. Hanson, R. Beattie, S. Varghese, T. M. D. Sennanayake, A. Hirata, F. Hirata, Y. Huang, Y. Wu, N. Steinbergs, T. Murray-Stewart, I. Bytheway, J. Casero, R.A. and P. M. Woster, *MedChemComm* 2012, **3**, 14.
25. S. Hazeldine, B. Pachaiyappan, N. Steinbergs, S. Nowotarski, A. S. Hanson, R. A. Casero, Jr. and P. M. Woster, *J Med Chem* 2012, **55**, 7378.
26. F. Forneris, C. Binda, A. Adamo, E. Battaglioli and A. Mattevi, *J. Biol. Chem.* 2007, **282**, 20070.
27. I. R. Kumarasinghe and P. M. Woster, *ACS Med. Chem. Lett.* 2014, **5**, 29.
28. http://www.oryzon.com/files/NdP2014/PRESS_RELEASE_01-2014def.pdf.
29. M. N. Khan, T. Suzuki and N. Miyata, *Med. Res. Rev.* 2013, **33**, 873.
30. Y. C. Duan, Y. C. Ma, E. Zhang, X. J. Shi, M. M. Wang, X. W. Ye and H. M. Liu, *Eur.J. Med. Chem.* 2013, **62**, 11.
31. Y. C. Duan, Y. C. Zheng, X. C. Li, M. M. Wang, X. W. Ye, Y. Y. Guan, G. Z. Liu, J. X. Zheng and H. M. Liu, *Eur.J. Med. Chem.* 2013, **64**, 99.
32. Y. C. Zheng, Y. C. Duan, J. L. Ma, R. M. Xu, X. Zi, W. L. Lv, M. M. Wang, X. W. Ye, S. Zhu, D. Mobley, Y. Y. Zhu, J. W. Wang, J. F. Li, Z. R. Wang, W. Zhao and H. M. Liu, *J. Med. Chem.* 2013, **56**, 8543.